Author 1

First name or initial	Middle name or initial	Surname	Suffix (Jr., III, etc.)	Role (job title, etc.)	Email (and phone for contact author)	Contact author? yes or no
Suman		Budhathoki		Graduate student	Szb0153@auburn.edu (3345910159)	Yes

Affiliation for Author1

Organization	Address	Country	URL or other info.
Auburn University	301 Corley Building, Auburn, AL 36849	USA	http://www.eng.auburn.edu/bsen/faculty/grad-dir.html

Author 2

First name or initial	Middle name or initial	Surname	Suffix (Jr., III, etc.)	Role (job title, etc.)	Email (and phone for contact author)	Contact author? yes or no
Jasmeet		Lamba	Dr.	Assistant Professor	Jsl0005@auburn.edu	no

Affiliation for Author 2

Organization	Address	Country	URL or other info.
Auburn University	228 Corley Building, Auburn, AL 36849	USA	http://www.eng.auburn.edu/bsen/faculty/index.html

Author 3 (repeat Author and Affiliation tables for each author)

First name or initial	Middle name or initial	Surname	Suffix (Jr., III, etc.)	Role (job title, etc.)	Email (and phone for contact author)	Contact author? yes or no
Puneet		Srivastava	Dr.	Professor	srivapu@umd.edu	no

Affiliation for Author 3

Organization	Address	Country	URL or other info.
University of Maryland	1201 Symons Hall Street 7998 Regents Drive, College Park, MD 20742-3131	USA	https://agnr.umd.edu/about/directory/puneet-srivastava

Author 4 (repeat Author and Affiliation tables for each author)

First name or initial	Middle name or initial	Surname	Suffix (Jr., III, etc.)	Role (job title, etc.)	Email (and phone for contact author)	Contact author? yes or no
Kritika		Malhotra		Graduate Student	Kzm0063@auburn.edu	no

Affiliation for Author 4

Organization	Address	Country	URL or other info.
Auburn University	309 Corley Building, Auburn, AL 36849	USA	http://www.eng.auburn.edu/bsen/faculty/grad-dir.html

Author 5 (repeat Author and Affiliation tables for each author)

First name or initial	Middle name or initial	Surname	Suffix (Jr., III, etc.)	Role (job title, etc.)	Email (and phone for contact author)	Contact author? yes or no
Thomas	R	Way	Dr.	Agricultural	Tom.way@usda.gov	no

				Engineer		

Affiliation for Author 5

Organization	Address	Country	URL or other info.
USDA-ARS National Soil Dynamics Lab	411 S. Donahue Dr., Auburn, AL 36832	USA	http://www.eng.auburn.edu/directory/twb0001

Author 6 (repeat Author and Affiliation tables for each author)

First name or initial	Middle name or initial	Surname	Suffix (Jr., III, etc.)	Role (job title, etc.)	Email (and phone for contact author)	Contact author? yes or no
Sheela		Katuwal	Dr.	Postdoctoral Fellow	skatuwal@uark.edu	no

Affiliation for Author 6

Organization	Address	Country	URL or other info.
University of Arkansas	Fayetteville, AR 72701	USA	https://poultry-science.uark.edu/people/staff.php

Using X-ray Computed Tomography to Quantify Variability in Soil Macropore Characteristics in Pastures

Highlights

- Macropore characteristics were quantified in pastures.
- Soils at 0-100 mm depth of the downslope location were susceptible to compaction.
- Preferential flow may be more restrictive in the downslope soils.
- Larger diameter cores can help provide representative macropore measurements.

Abstract. *Soil macropores largely control the transport phenomenon of water and solutes in subsurface flows. Preferential flow via soil macropores can substantially affect water quality. Hence, it is important to quantify soil macropore characteristics and link this information with the preferential flow behavior in soils. However, whether macropore structure at one slope position within a field is different than that at another is unclear. With differences in the macropore characteristics, each slope position can contribute differently to the runoff and subsurface flows. The objective of this study was to use X-ray CT and image analysis to characterize soil pore structure at upslope, midslope, and downslope positions within a 0.40 ha pasture field. A total of 18 undisturbed soil columns (150 mm diameter and 500 mm depth) were collected from a pasture field located at the Sand Mountain Research and Extension Center, Alabama, during May 2019. The results indicated that both the macropore number and macroporosity values were lowest at the downslope position in the 0-100 mm soil layer. In contrast, a large number of macropores was observed at the downslope soils for depths below 200 mm. The lowest macroporosity values in the surface layer at the downslope position can be attributed to higher soil moisture content at the downslope location, via runoff and seepage losses from the upper slopes. This resulted in higher degree of compaction due to trampling by cattle. Macropore interconnectivity at the subsurface layer (100-500 mm) increased from the upslope to the downslope position, whereas at the soil surface (0-100 mm), the interconnectivity was lowest at the downslope position as compared to the upslope and midslope locations. These provide quantitative information of different soil macropore characteristics under varying topographical locations and depths in a pasture field.*

Keywords. *X-ray Computed Tomography; Preferential flow; Compaction; Pasture; Macropores*

INTRODUCTION

In recent years, there has been an increasing interest to understand loss of pollutants via subsurface flow pathways, specifically in areas where subsurface flows are significant (McGrath et al., 2010). Soil macropores play an important role in the movement of water and agrochemicals through the soil profile. Although, macropores represent only a small fraction of the overall soil porosity, they can result in transport of fertilizers and other contaminants to relatively deep depths in soil and even to the groundwater (Jarvis, 2007). Preferential flow via soil macropores in the presence of an impermeable soil layer can result in transport of surface applied fertilizers and other chemicals to relatively long distances within a watershed (Wang et al., 2011). In certain soils, preferential flows can contribute to the transport of more than 90% of water and contaminants (Shaffer et al., 1979). For example, a study in the Walker Branch watershed in eastern Tennessee reported that preferential flow through mesopores and macropores was the predominant mechanism of streamflow generation (Wilson et al., 1990). Therefore, quantification of macropores characteristics can improve our understanding of preferential flows and help develop a reasonable mathematical model (Zhang et al., 2017).

Topographical differences at a field level exert a strong control on soil properties including bulk density, moisture content, and organic matter content, which in turn may contribute to the variation in soil macropores (Hao et al., 2002; Oztas et al., 2003). A small difference in topography can cause major changes in soil development (Rezaei and Gilkers, 2005). Soil properties including moisture content and organic matter content, which are primarily influenced by the topography, promote the formation and stabilization of larger pores in the soil (Grosbellet et al., 2011; Holden, 2009). For example, in a grazed pasture field, macroporosity of the surface soil is influenced by the soil water content, which affects the degree of compaction by trampling. Continuous grazing of pastures can cause reduction in topsoil porosity (Singleton et al., 2000) and vertical pore continuity (Greenwood and McKenzie, 2001) through the disruption of large aggregates and repacking with smaller aggregates to fill existing soil pores

(Cattle and Southorn, 2010). Macropore structure damage by such compaction commonly occurs in surface layers and decreases with depth (Drewry et al., 2008). Warren et al. (1986) suggested that the impact of livestock trampling is generally more significant with higher soil moisture content at the time of trampling. However, limited work has been done to investigate how distribution of macropores will change as a result of topography.

X-ray computed tomography (CT) is a relatively new and promising approach to understand the configuration of soil pores in the soil profile (Rab et al., 2014; Luo et al., 2010). A major advantage of this method is that it is non-destructive and can help quantify macropores in 3-D (Helliwell et al., 2013). Other methods, such as dye tracers (e.g., Wahl et al., 2004), resin impregnation (Singh et al., 1991), and tension infiltrometer (e.g., Mohanty et al., 1996; Cameira et al., 2003) have also been widely used for studying macropores in the past. However, measurements of macroporosity using the above-mentioned methods are indirect, time-consuming, and less accurate in reflecting the subtle features of the soil pore networks (Amer et al., 2009; Matthews et al., 2010). Nonetheless, CT techniques have been successfully used to determine the number, size, and distribution of macropores (Warner et al., 1989; Rab et al., 2014; Luo et al., 2010).

Quantification of macropore characteristics in soils where subsurface flows are substantial is important to understand pollutant transport processes. In the Sand Mountain region of north Alabama, which is a major poultry-producing region, excessive buildup of P in soils and contamination of surface water bodies with P has been a serious issue due to the continuous application of poultry litter to the pastures (Sen et al., 2008). Sen et al. (2008) ascertained that both the surface and subsurface runoff generation mechanisms could be responsible for the off-site transport of contaminants in this region. Also, results of a study conducted by Lamba et al. (2012) show that less than 10% of rainfall contributed to surface runoff and more than 90% infiltrated into the soil, suggesting that there are significant subsurface flows in this area. Therefore, it is very important to understand the macropore characteristics in this region to elucidate subsurface flow mechanisms. Up to now, only one study conducted by Zong-Chao Li et al.

(2019) has used CT to study the influence of topography on soil macropore characteristics which demonstrated a clear distinction among three slope positions in an alpine meadow. No study has been reported so far that uses CT to quantify soil macropore characteristics for enhanced understanding of the complex interaction between soil pore space and the topographical position in pastures. Therefore, the objective of this study was to quantify the soil macropore characteristics in different soil layers and slope positions of a pasture field using CT.

MATERIALS AND METHODS

STUDY SITE

The soil columns investigated in this study were excavated from a hillslope pasture field (34°17'02.6"N, 85°57'51.8"W) located at the Sand Mountain Research and Extension Center (SMREC) in north Alabama at an elevation of about 350 m above the mean sea level. The site where the study was conducted is an approximately 0.40 ha with a slope length of 80 m. The site had been grazed by cattle for more than 15 years prior to sampling. The slope of the site was 3.4%. The soil at study site is a Hartsells (Fine-loamy, siliceous, subactive, thermic Typic Hapludults). This soil is well drained with moderate permeability, primarily with slopes between 3 and 8% on broad smooth plateaus, mountaintops, or hilltops. The parent material of the soil is loamy residuum weathered from sandstone and shale (Soil Survey Staff, 2020). Based on an analysis of 30-year normals, mean annual precipitation in this region is 1340 mm, and the mean annual temperature is 14.8 °C. A cool-season grass (Kentucky 31 Tall Fescue (*Festuca arundinacea Schreb*)) has been growing at the study site for more than 40 years. This grass has an extensive root system which extends to a depth of 900 mm below the soil surface, providing access to water and other resources, and offers better heat and drought tolerance than many other cool-season grasses (Cougnon et al., 2017).

SOIL SAMPLING

A total of 18 undisturbed soil columns (150 mm diameter, and 500 mm depth) were collected in May 2019. Six cores were collected from each of three topographical locations (upslope, midslope, and downslope) within the field. The samples were obtained using rigid PVC pipes driven carefully into the soil by utilizing a tractor-mounted soil coring system (Prior et al., 2004). After sampling, the airspace at each end of each soil column in PVC pipe was filled with bubble wrap packing material, and a PVC end cap was fitted over each end of the pipe before transportation. During transportation, a 150 mm thick layer of wood shavings supported the soil columns to serve as cushioning, to minimize disturbance of the soil columns. The samples were then stored at 4 °C until further analysis. In addition to the 18 cores, two extra soil columns were collected from the field, to allow us to make artificial soil pores of known diameter in the soil. These cores were later used as a reference to allow us to distinguish between the pores and the rest of the soil matrix. Prior to scanning, all the soil columns were saturated with water and left to drain for about 3 days in order to maintain a uniform moisture condition among all cores. This was done to minimize the variability in the X-ray attenuation value histogram and to make the comparison between different slope positions more consistent (Luo et al., 2010).

Additional soil samples were collected from each topographical location at different depth intervals (0-100 mm, 100-200 mm, 200-300 mm, 300-400 mm, and 400-500 mm) for the analysis of routinely measured soil properties (e.g., bulk density, organic matter content, and texture) (Table 1). The sand, silt, and clay percentages of soils were determined using hydrometer method (Bouyoucos, 1962). Organic matter content was determined by the weight loss on ignition method. The soil bulk density was calculated as the mass of oven-dried soil divided by its volume.

Table 1. Mean (n = 3) soil organic matter (%), sand (%), silt (%), clay (%), and bulk density (g cm^{-3}) at different topographical locations (downslope (DS), midslope (MS) and upslope (US)). Values shown in parentheses are standard deviations.

Depth (mm) [a]	Slope position	Organic matter (%)	Sand (%) [b]	Silt (%) [b]	Clay (%)[b]	Dry bulk density (g cm^{-3})
0-100	DS	6.00 (±0.05) a	53.90 (±1.53) a	7.50 (±1.30) a	38.60 (±2.03) a	1.31 (±0.14) a
	MS	3.93 (±0.19) b	68.80 (±2.63) b	8.70 (±3.99) a	22.60 (±1.50) b	1.17 (±0.11) a
	US	4.75 (±0.28) c	58.00 (±0.12) a	9.20 (±1.23) a	32.80 (±1.33) a	1.10 (±0.07) a
100-200	DS	3.28 (±0.10) a	60.40 (±1.46) a	8.60 (±2.24) a	31.00 (±1.96) a	1.18 (±0.17) a
	MS	3.23 (±0.26) a	69.00 (±2.66) b	6.90 (±1.55) a	24.10 (±1.50) b	1.17 (±0.18) a
	US	3.28 (±0.12) a	59.5 0(±1.53) a	6.9 0(±0.04) a	33.60 (±1.49) a	1.22 (±0.11) a

200-300	DS	2.31 (±0.23) a	61.60 (±2.47) a	8.50 (±1.40) a	29.90 (±1.46) a	1.19 (±0.21) a
	MS	2.83 (±0.19) a	73.40 (±3.87) b	6.90 (±2.93) a	19.70 (±1.47) b	1.44 (±0.06) a
	US	2.65 (±0.33) a	61.90 (±3.11) a	8.10 (±2.57) a	30.00 (±0.72) a	1.39 (±0.04) a
300-400	DS	2.54 (±0.21) a	66.70 (±4.39) a	9.80 (±4.08) a	23.50 (±0.72) a	1.30 (±0.15) a
	MS	2.61 (±0.33) a	73.50 (±4.01) a	5.60 (±3.29) a	21.00 (±2.67) a	1.44 (±0.10) a
	US	2.98 (±0.26) a	66.10 (±2.72) a	6.90 (±1.30) a	27.10 (±1.49) a	1.35 (±0.05) a
400-500	DS	2.42 (±0.45) a	68.80 (±3.96) a	9.40 (±3.28) a	21.80 (±0.69) a	1.24 (±0.13) a
	MS	2.37 (±0.17) a	74.00 (±0.69) a	6.80 (±1.27) b	19.20 (±1.47) a	1.29 (±0.02) a
	US	2.52 (±0.15) a	68.40 (±1.52) a	7.70 (±1.51) a	23.90 (±0.01) a	1.35 (±0.12) a

[a] Within each depth, mean values of different soil properties followed by the same letter at different topographical positions are not significantly different at the 0.05 probability level.

[b] Textural classification was according to the USDA soil taxonomy; Measured by hydrometer method; Clay fraction < 0.002 mm, Silt fraction 0.05-0.002 mm, and Sand fraction 0.05-2 mm (Bouyoucos, 1962).

CT SCANNING AND IMAGE ANALYSIS

The soil cores were scanned using a medical GE LightSpeed VCT 64 Slice CT scanner (GE Healthcare, Chicago, IL) installed in the Bailey Small Animal Teaching Hospital at the Auburn University College of Veterinary Medicine (AUCVM). The machine has the ability to take up to 64 slices in one scan, thus, covering 40 mm at 0.625 mm slice thickness in one scan. The scanner was operated with the scanning parameters set to 140 KV, 140 mA, and 1 s exposure time, and this provided detailed projections with relatively little noise. The field of view (FOV) was set to 180 mm producing 16-bit 512x512 images with a voxel size of 0.35x0.35x0.625 mm^3.

These images were analyzed using the ImageJ version 1.52t software (Rueden et al., 2017), which is a digital image processing program developed by the US National Institutes of Health (Bethesda, MD). The software was used to determine the macropore number, macropore diameter (ECD), macroporosity, and inter-connectivity for each stack. To avoid voids near the core walls, the diameter of the core was reduced from 150 mm to 136 mm, and the area beyond this region of interest (ROI) was deleted by using the “clear outside” tool in ImageJ. The slices from the bottom of the core which were void or seemed to be disturbed were excluded from the original stack for analysis. After adjusting the brightness and contrast of the images, a *median filter* with a radius of 1 pixel was used to reduce noise in the images. The “Unsharp mask” command with its default values (radius of 1 pixel and mask weight of 0.6) was used to sharpen and enhance the edges.

The images were segmented using Phansalkar's method of local thresholding which is a modification of Sauvola's thresholding method to deal with low contrast images (Phansalkar et al., 2011). All the images were converted to 8-bit before performing this operation. The threshold value T for the 8-bit images were then calculated as:

$$T = mean * (1 + p * \exp(-q * mean) + k * ((stdev / r) - 1)) \quad (1)$$

Where, mean and stdev are the local mean and standard deviation for a selected window size, respectively. The parameters k and r which can be adjusted to get the best segmentation results, were set to their default values in the ImageJ software ($k = 0.25$ and $r = 0.5$). The values of parameters p and q were 2 and 10, respectively and are fixed in the plugin. The segmentation was carried out using a radius of 5 pixels over which the threshold was computed. All the images were visually inspected for the performance of the segmentation procedure in separating the pores and solids. To determine the parameters of thresholding (i.e., k, r, and the radius), Plexiglas thermoplastic cylinders of two different diameters (3.17 mm and 4.76 mm) were inserted into an undisturbed soil column to create artificial macropores. The Plexiglas rods were pulled out just before CT scanning. The macropore size of the artificial pores with known diameter based on image analysis was compared with the actual pore size for different randomly selected thresholding parameter values. A parameter value was selected if the difference between the actual and the image-analyzed pore size was less than 1.5% for both rod diameters.

The binary images were then analyzed using the "Analyze Particles" tool in ImageJ to determine the number of pores and pore area in a 2-D representation of a slice. Since the pixel resolution was 0.35 mm * 0.35 mm, only those pores with equivalent cylindrical diameter (ECD) greater than twice the resolution i.e., 0.70 mm could be reliably identified using the image processing method. The equivalent cylindrical diameter was calculated based on the surface area using the equation: $ECD = 2(area/\pi)^{0.5}$. We considered pores with ECD >0.75 mm as macropores in this study, similar to Luo et al. (2008) and Luo et al. (2010). This was done to ensure that we were not quantifying any noise as pores in our analyses. All the pores with ECD smaller than 0.75 mm were considered as noise and removed from the analysis. The number of macropores, diameter, and macroporosity were calculated for each slice and then averaged to quantify the variation with depths. Macropores, especially with diameter (ECD) > 1 mm, promote water movement through the soil profile (Udawatta et al., 2008). Node density, which is the sum of the number of nodes where at least two pore branches connect per unit volume of soil considered, was used to quantify the interconnectivity of the macropores (Luo et al., 2010). A high node density of junctions is related to an extensive and well-connected pore network (Munkholm et al., 2012). For this, the BoneJ plug-in (Doube et al., 2010) in the ImageJ software was used.

All the pores were divided into three pore-size classes: pores with ECD greater than 0.75 mm and less than 1 mm, all pores with ECD greater than 0.75 mm, and those greater than 1 mm. Thus, both macroporosity and number of pores were determined for these pore classes. The total pore area covered by pores <1 mm, >0.75 mm, and >1 mm was divided by the total ROI, i.e., 14527 mm^2 to estimate the macroporosity. In addition, depth to the most restrictive layer was determined for each soil column. For this, macroporosity of each slice perpendicular to the column axis (0.625 mm thickness) along the length of the column was calculated. The slice with least macroporosity was defined as the limiting layer for any particular soil column.

STATISTICAL ANALYSIS

All statistical analyses were performed using SAS version 9.4 (SAS Institute, USA). The significance test for the effects of slope position on different soil characteristics was done using one-way analysis of variance (ANOVA) within the General Linear Model (GLM) procedure. The Tukey's multiple comparison test was used to compare the soil characteristics as a function of soil depth and topographic location. A repeated measures analysis with PROC MIXED was used to account for correlation between measurements within the same sample. All statistical tests were conducted at the 95% confidence level.

Results and Discussion

Quantification of Macropore Networks

The spatial macropore characteristics were distinctly different for the different slope positions. In the surface layer (0 to 100 mm), the macropores were relatively larger and highly continuous at all the slope positions (Table 2). These macropores were likely formed by root channels and earthworm burrows, whereas smaller and separated macropores just below the surface soil layer were probably the inter-aggregate pores (Luo et al., 2008). In addition, all the soil columns had relatively less macroporosity in the 100-200 mm depth layer. This is consistent with the findings of Sen et al. (2008) who reported presence of a restrictive layer near the surface soil at the study site. This restrictive layer was responsible for the formation of a perched water table during intense rainfall events. Most of the macropores at the downslope location were concentrated in the deep soil layers (250-500 mm). The macropores at the upslope locations were comparatively well distributed throughout the entire depth of the soil column. Quantitative data on the soil macropore characteristics are presented in Table 2.

During soil sampling, we observed earthworms and some termites in the surface layer of the downslope soils but not at the other two slope positions. However, we observed a highly developed root system in the midslope soil columns that can be attributed to the presence of thick and tubular macropores in the midslope columns. For all the slope positions, the soil condition 50-100 mm below the surface, made it relatively difficult to push the PVC pipe down through the soil. This was probably due to the presence of a restrictive layer, as observed by Sen et al. (2008).

Table 2. Average (n = 6) number of macropores, average macropore diameter, and average macroporosity, in the US (upslope), MS (midslope), and DS (downslope) locations determined using computed tomography.

Slope position	Number of macropores (mean ± SD) [b]	Macropore size (mean ± SD) [b]	Macroporosity (%) (mean ± SD) [b]	Mean macropore diameter (mm) (mean ± SD) at different depths [a]				
				0-100 mm	100-200 mm	200-300mm	300-400 mm	400-500 mm
DS	135 (±14) a	1.65 (±0.09) a	3.39 (±0.32) a	2.11 (±0.27) a	1.39 (±0.09) a	1.41 (±0.07) a	1.62 (±0.13) a	1.68 (±0.18) a

MS	115 (±14) a	1.63 (±0.15) a	3.00 (±1.04) a	1.92 (±0.10) ab	1.55 (±0.15) a	1.50 (±0.17) a	1.55 (±0.23) a	1.60 (±0.29) a
US	130 (±18) a	1.57 (±0.07) a	2.77 (±0.37) a	1.80 (±0.15) b	1.45 (±0.12) a	1.47 (±0.07) a	1.45 (±0.08) a	1.48 (±0.05) a

[a] Within each depth, values followed by the same letter are not significantly different at the 0.05 probability level.
[b] Mean values of different properties followed by the same letter at different topographical positions are not significantly different at the 0.05 probability level. Data in the parentheses are standard deviations (n = 6). DS = Downslope position; MS = Midslope position; US = Upslope position

DISTRIBUTION OF MACROPOROSITY AND NUMBER OF MACROPORES IN DIFFERENT SOIL LAYERS AND SLOPE POSITIONS

The number of soil macropores followed similar trends for all the macropore size classes at all the topographical locations (Figure 1). However, for >1 mm, the number of macropores, was less in the 100-200 mm depth layer compared to the 0-100 mm layer. The number of macropores <1 mm showed a gradual increase with the depth. Significant differences (P<0.05) were found in the number of soil macropores at different topographical locations for a given depth (Figure 1). For example, in the shallow soil layer (0-100 mm), the number of macropores for all size classes was significantly less (P<0.05) for the downslope location than the midslope and upslope locations. However, at the deeper soil depths (e.g., 200-300 and 300-400 mm), the number of macropores at the downslope location was significantly greater (P<0.05) than either the upslope or midslope location.

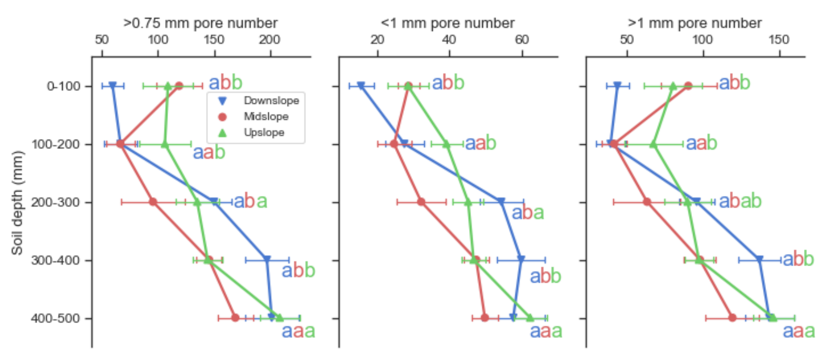

Figure 1. Effects of slope position on number of >0.75 mm soil pores, >1 mm soil pores, and <1 mm soil pores as a function of soil depth. Error bars indicate the standard deviation (n=6).
Within each depth, different letters for the slope positions (represented by different colors) indicate significantly different values at the 0.05 probability level.

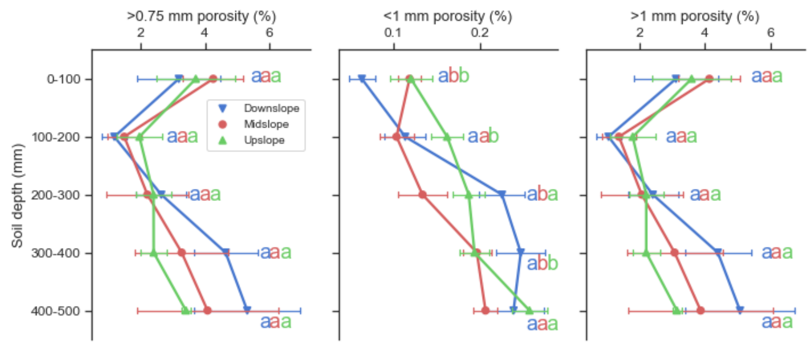

Figure 2. Effects of slope position on the >0.75 mm soil porosity, >1 mm soil porosity, and <1 mm soil porosity in different soil layers. Error bars indicate standard deviation (n=6).
Within each depth, different letters for the slope positions (represented by different colors) indicate significant difference at the 0.05 probability level.

The soil macroporosity of >0.75 mm and >1 mm soil pores first declined sharply with increasing depth down to 200 mm and then increased gradually at all the slope positions, whereas a general increase with depth was observed for <1 mm soil pores (Figure 2). The sharp decline in macroporosity values from the first soil layer (0-100 mm) to the second soil layer (100-200 mm) for all the topographical locations can be attributed to both the rooting characteristics of Kentucky-31 tall fescue. In a study of relative rooting depth for different grasses, Brown et al. (2010) reported that more than 65% of the root mass of tall fescue (F. Arundinacea) was distributed within the top 75 mm of the soil profile, whereas around 75% of the root mass was observed within the top 150 mm depth. In our results, significant differences ($P<0.05$) in macroporosity among the three topographical locations were observed only for <1 mm pores. In the shallow soil layers (0-100 mm and 100-200 mm), macroporosity of <1 mm soil pores at the downslope location was significantly ($P<0.05$) lower than that of the upslope location. The distribution of the macroporosity values for the three topographical locations corresponded well with the number of macropores. Significantly lower values of the number of macropores, and macroporosity of <1 mm pores at the surface layer (0-100 mm) at the downslope location, were probably due to a combination of compaction caused by cattle grazing (Luo et al., 2010) and greater soil moisture content expected at the downslope location compared to other topographical locations. Oztas et al. (2003) reported a higher degree of compaction at the downslope location of a grazed hillslope, due to higher soil moisture contents of downslope locations compared to upslope locations. We speculate that, runoff and seepage from the upper slopes might have caused higher moisture content at the downslope location, and this increased the degree of compaction at the downslope location, caused by animal trampling. Also, greater clay content, 38.6%, at the downslope location (0-100 mm), compared to 22.6% at the midslope, and 32.8% at the upslope location, might have been responsible for maintaining relatively high water content at the downslope location, thereby facilitating compaction due to grazing (Table 1). This was consistent with the bulk density results (0-100 mm), which showed a relatively higher bulk density value at the downslope, 1.31 g cm^{-3}, compared to 1.17 g cm^{-3} and 1.10 g cm^{-3} at the midslope and upslope locations, respectively (Table 1). Similarly, Zong-Chao Li et al. (2019) observed a decrease in average soil macroporosity in the surface layer (0-100 mm) from the upper slopes to the downslope location. No significant differences ($P>0.05$) between the slope positions were noted for macroporosity due to pores >1 mm in the surface layer (0-100 mm). This result suggests that pores larger than 1 mm were probably less susceptible to compaction due to grazing compared to pores less than 1 mm in size. Conversely, at the downslope locations, compaction effects in the surface soil layer (0-100 mm) have been counteracted by the presence of biologically more active soils in the downslope that facilitated formation of relatively larger macropores (Luo et al., 2010). Similarly, mean macropore diameter at the surface layer (0-100 mm) of the downslope location was significantly higher as compared to the soils of the upslope location ($P<0.05$; Table 2).

The average macroporosity determined for this pasture field ranged from 2.77 ± 0.37 % at the upslope to 3.39 ± 0.32 % at the downslope position (Table 2). These values found in our study are comparable with Luo et al. (2010), which reported an average macroporosity of 3.1 % for a fine-loamy soil under pasture. Luo et al. (2010) quantified macropores as pores with ECD > 0.75 mm, similar to that of our present study. Therefore, results of this study are in agreement with the Luo et al. (2010). Furthermore, Perret et al. (1998) reported macroporosity between 2.1 % and 3.8 % taken from the top 800 mm of a sandy loam soil under grassed field borders. Muller et al. (2018) observed a decreasing macroporosity with depth under a permanent pasture grazed by cattle, and reported an average macroporosity of 6%, which is higher than the values reported in our study. This is due to the fact that they considered pores greater than or equal to 0.147 mm diameter in their analysis. Moreover, the trend of macroporosity variation with depth found in our study is consistent with the results of Perret et al. (1998) and Hu et al. (2015), who observed a sharp decrease in macroporosity for depths to 200 mm and then macroporosity values increased as the depth increased to 500 mm in grasslands. These fluctuations in the soil macropore characteristics within the 0-500 mm soil depth clearly indicate the importance of using deeper cores to accurately represent the overall macropore structure in an agricultural field. Thus, it is important to consider the depth of soil sampling used in a particular study before making any important comparisons of the soil macropore characteristics. Overall, results indicate that soil macropores are prevalent in this region and therefore can be important pathways for subsurface flows potentially resulting in substantial off-site transport of pollutants. Sen et al. (2008) reported that out of 26 rainfall events monitored at this study site from January 2006 to January 2007, only 8 storm events generated surface runoff. Furthermore, Lamba et al. (2012) reported that more than 90% of the rainfall infiltrates in this region and subsurface flows could be important pathway for pollutant transport. Hence, results of our study in conjunction with Sen et al (2008) and Lamba et al. (2012) indicate that soil macropores play an important role in generation of subsurface flows in this region.

LIMITING MACROPOROSITY AT DIFFERENT SLOPE POSITIONS

Flow and contaminant transport are strongly restricted at the "bottlenecks" in soil profile; thus, quantifying the position and macroporosity of this limiting layer is important in understanding the soil hydraulic properties (Katuwal et al., 2015, Zhang et al., 2019). The depth to limiting macroporosity at different topographical positions is presented in Figure 3. At the downslope location, the restricting depths were present from 100 to150 mm, with an average limiting macroporosity value of 0.27%. The restricting depths at the upslope location were also observed within the top 150 mm of soil depth; for two cores the restricting depths were at 60 and 63 mm, while for the other four, the depth ranged from 120 to 150 mm. The limiting macroporosity values for soils at the upslope locations were clearly higher than those at the downslope location. For all the soil columns from the midslope location, the limiting macroporosity values were observed at deeper depths (>150 mm) and the macroporosity values were much higher as compared to the soil at the downslope location. In summary, because the slope location with the most limiting macroporosity values is the downslope location, preferential water flow is likely to be less at the downslope location compared to the midslope and upslope locations. This result is consistent with the study conducted by Zong-Chao Li et al. (2019), who observed that water can move preferentially through soil macropores (ECD ≥ 1 mm) on the upper and middle slopes, compared to the bottom slope of a silty loam soil under an Alpine meadow. For all the soil cores, the depth to restricting macroporosity was closer to the soil surface at the downslope location as compared to the other topographical locations.

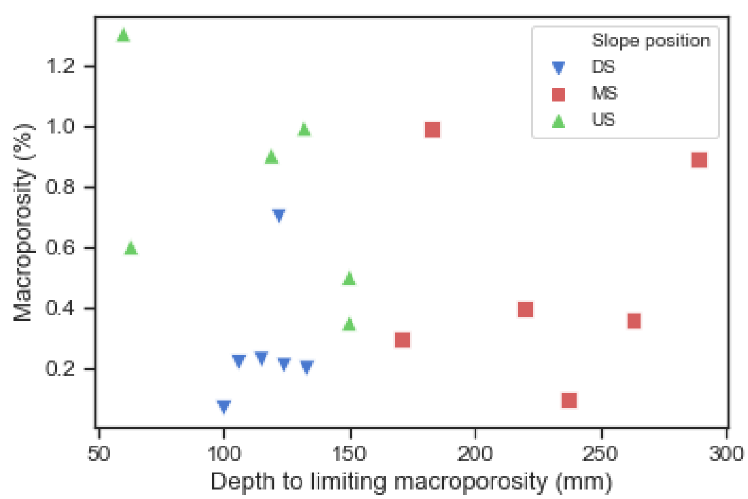

Figure 3. Position of the limiting macroporosity in all the samples (n=18) of upslope, midslope and downslope locations. Limited macroporosity is based on each individual slice sampled at 0.625 mm intervals.

MACROPORE CONNECTIVITY AT DIFFERENT SLOPE POSITIONS

Inter-connectivity, quantified using the node density of macropores, indicated there was a significant effect ($P<0.05$) of depth on the macropore interconnectivity in the soils at the downslope position (Figure 4). The inter-connectivity of the surface soil (0-100 mm) at the downslope location was significantly less ($P<0.05$) as compared to the subsurface (100-500 mm) interconnectivity, whereas no significant ($P>0.05$) reduction in interconnectivity was seen in the surface soil layer (0-100 mm) at the upslope and midslope locations. In contrast to the soil at the downslope location, the soil at the midslope and upslope locations had a higher interconnectivity in the surface soil layer (0-100 mm) than in the subsurface (100-500 mm). Overall, subsurface interconnectivity increased from the upslope towards the downslope location. In addition to macroporosity, macropore diameter, macropore number, and connectivity are key variables that affect the transport phenomenon in soil (Hu et al., 2018; Katuwal et al., 2015). High node density in soil is related to highly connected root networks and movement of earthworms and other organisms in the soil profile which promote the preferential flow phenomenon. Higher degrees of interconnectivity among the macropores in the downslope (Figure 4) could be related to favorable conditions for biota activities in the soil at the downslope location. However, significantly less interconnectivity at the surface (0-100 mm) of the downslope as compared to its subsurface interconnectivity (Figure 4) can be attributed to trampling effects of the cattle along with the high soil moisture content. Hence, we expect a higher preferential flow through the macropores of the upslope and midslope locations, with less vertical movement through soils at the downslope location. The soil at the downslope location might contribute to more surface flow as a result of its highly compacted surface layer (0-100 mm) (Figure 1 and Figure 2) which has significantly less interconnected pores. Moreover, limiting macroporosity, which was observed within the top 150 mm at the downslope location, was substantially lower as compared to the midslope and upslope soils. This will limit preferential flow at the downslope location, compared to the upslope and midslope locations. Results of this study highlight the importance of considering variability in macropore characteristics within a field.

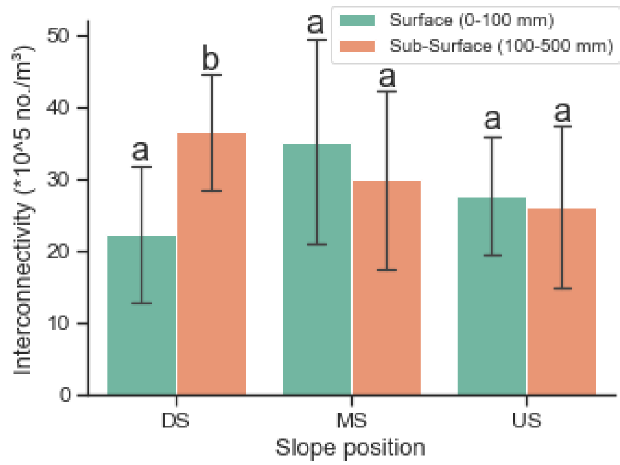

Figure 4. Interconnectivity of surface macropores (0-100 mm) as compared to the subsurface interconnectivity (100-500 mm) at different topographical positions in a pasture. Within each slope position, different letters indicate a significant difference in interconnectivity (node density) between the surface and subsurface soil depth (P<0.05).

IMPLICATIONS OF MACROPORE CHARACTERISTICS FOR FLOW AND CONTAMINANT TRANSPORT

Macropores are large pores that freely drain under gravity and often contribute more than 70% of the total soil water infiltration (Watson and Luxmoore, 1986; Hirmas et al., 2018). Numerous studies in the past have demonstrated that the presence of soil macropores results in rapid downward movement of contaminants which may lead to groundwater and surface water pollution. Quantification of macropore characteristics help provide a better understanding of fate and transport processes of contaminants within the soil profile (Mooney and Morris, 2008; Jarvis et al., 1991). Borah et al. (1999) reported an improvement in the predictive capability of a solute leaching model (LEACHM) with the addition of a macropore flow component.

The differences in macropore characteristics among the different slope positions and depths imply that the soil hydraulic properties vary as a function of topographical location in a pasture field. Because of the presence of macropores, contaminants may quickly bypass the soil profile and reach groundwater or nearby surface water through subsurface flows. Based on results of this study, it is expected that macropores would play a more prominent role in contaminant transport at the upslope and midslope locations, as compared to the downslope area. Despite high overall macroporosity observed for downslope samples, surface interconnectivity (0-100 mm) and surface macroporosity (0-100 mm) were negatively influenced by the compaction effects. The connectivity of macropores affects their capacity to transport water and chemicals in the soil profile (Gerke et al., 2015). In addition, it can be expected that preferential flow would be more restrictive in the downslope soil because of lower values for limiting macroporosity near the soil surface. These macropore characteristics need to be linked to soil hydraulic properties to better understand the flow and contaminant transport processes and develop appropriate management practices.

CONCLUSIONS

The study quantified variation in soil macropore characteristics at different depths at upslope, midslope, and downslope locations within a pasture field. The results show a clear and consistent evidence that macropore characteristic variation within the field was not random but indeed linked to the topographical position in the field. Similarly, topography influenced macropores of different sizes. For pores smaller than 1 mm diameter, both mean macropore number and macroporosity were significantly lower at the downslope location, at the surface layer (0-100 mm), compared to the soils at the upslope and midslope locations at the same depth. However, no significant differences were seen between the three topographical positions for the overall macroporosity (>0.75 mm porosity) at any depths. Lower macroporosity and macropore number values were observed at downslope positions as compared to the other slope positions in the top 100 mm. This likely resulted from high soil moisture content along with trampling by grazing animals at the downslope location compared to upslope and midslope locations. In addition, architecture of the plant roots plays an important role in variation of macropore characteristics. Further research is required for evaluating the variability of pores <0.75 mm in diameter using higher resolution CT scanner and smaller soil cores.

ACKNOWLEDGEMENTS

This work was supported by the USDA-NIFA award # 2018-67019-27806, USDA-NIFA Hatch Project (ALA014-1-19052), and the Alabama Agricultural Experiment Station. We thank Marlin R. Siegford, Peyton Heath, Thomas Counts, Takhellambam Bijoychandra Singh, and staff at the Sand Mountain Research and Extension Center for assistance in this research project.

REFERENCES

Amer, A.M.M., Logsdon, S.D., Davis, D., 2009. Prediction of hydraulic conductivity as related to pore size distribution in unsaturated soils. Soil Sci. 174, 508–515. https://doi.org/10.1097/SS.0b013e3181b76c29

Borah, M. J., and Kalita P. K. 1999. Development and evaluation of a macropore flow component for LEACHM. Trans. ASABE 42, 65–78.

Bouyoucos, G.J., 1962. Hydrometer Method Improved for Making Particle Size Analyses of Soils 1 . Agron. J. 54, 464–465. https://doi.org/10.2134/agronj1962.00021962005400050028x

Brown, R.N., Percivalle, C., Narkiewicz, S., DeCuollo, S., 2010. Relative rooting depths of native grasses and amenity grasses with potential for use on roadsides in New England. HortScience 45, 393–400. https://doi.org/10.21273/hortsci.45.3.393

Cameira, M.R., Fernando, R.M., Pereira, L.S., 2003. Soil macropore dynamics affected by tillage and irrigation for a silty loam alluvial soil in southern Portugal. Soil Tillage Res. 70, 131–140. https://doi.org/10.1016/S0167-1987(02)00154-X

Cattle, S.R., Southorn, N.J., 2010. Macroporosity of pasture topsoils after three years of set-stocked and rotational grazing by sheep. Aust. J. Soil Res. 48, 43–57. https://doi.org/10.1071/SR09004

Cougnon, M., De Swaef, T., Lootens, P., Baert, J., De Frenne, P., Shahidi, R., Roldán-Ruiz, I., Reheul, D., 2017. In situ quantification of forage grass root biomass, distribution and diameter classes under two N fertilisation rates. Plant Soil 411, 409–422. https://doi.org/10.1007/s11104-016-3034-7

Doube, M., Klosowski, M.M., Arganda-Carreras, I., Cordelières, F.P., Dougherty, R.P., Jackson, J.S., Schmid, B., Hutchinson, J.R., Shefelbine, S.J., 2010. BoneJ: Free and extensible bone image analysis in ImageJ. Bone 47, 1076–1079. https://doi.org/10.1016/j.bone.2010.08.023

Drewry, J.J., Cameron, K.C., Buchan, G.D., 2008. Pasture yield and soil physical property responses to soil compaction from treading and grazing - A review. Aust. J. Soil Res. 46, 237–256. https://doi.org/10.1071/SR07125

Gerke, K.M., Sidle, R.C., Mallants, D., 2015. Preferential flow mechanisms identified from staining experiments in forested hillslopes. Hydrol. Process. 29, 4562–4578. https://doi.org/10.1002/hyp.10468

Greenwood, K.L., and B.M. McKenzie. 2001. Grazing effects on soil physical properties and the consequences for pastures: A review. Aust. J. Exp. Agric. 41, 1231-1250.https://doi.org/10.1071/EA00102

Grosbellet, C., Vidal-Beaudet, L., Caubel, V., Charpentier, S., 2011. Improvement of soil structure formation by degradation of coarse organic matter. Geoderma 162, 27–38. https://doi.org/10.1016/j.geoderma.2011.01.003

Hao, Y., Lal, R., Owens, L.B., Izaurralde, R.C., Post, W.M., Hothem, D.L., 2002. Effect of cropland management and slope position on soil organic carbon pool at the North Appalachian Experimental Watersheds. Soil Tillage Res. 68, 133–142. https://doi.org/10.1016/S0167-1987(02)00113-7

Helliwell, J.R., Sturrock, C.J., Grayling, K.M., Tracy, S.R., Flavel, R.J., Young, I.M., Whalley, W.R., Mooney, S.J., 2013. Applications of X-ray computed tomography for examining biophysical interactions and structural development in soil systems: A review. Eur. J. Soil Sci. 64, 279–297. https://doi.org/10.1111/ejss.12028

Hirmas, D.R., Giménez, D., Nemes, A., Kerry, R., Brunsell, N.A., Wilson, C.J., 2018. Climate-induced changes in continental-scale soil macroporosity may intensify water cycle. Nature 561, 100–103. https://doi.org/10.1038/s41586-018-0463-x

Holden, J., 2009. Topographic controls upon soil macropore flow. Earth Surf. Process. Landforms 34, 613–628. https://doi.org/10.1002/esp

Hu, X., Li, Z., Li, X., Wang, P., Zhao, Y., Liu, L., Lu, Y., 2018. Soil Macropore Structure Characterized by X-Ray Computed Tomography Under Different Land Uses in the Qinghai Lake Watershed, Qinghai-Tibet Plateau. Pedosphere 28, 478–487. https://doi.org/10.1016/S1002-0160(17)60334-5

Hu, X., Li, Z.C., Li, X.Y., Liu, Y., 2015. Influence of shrub encroachment on CT-measured soil macropore characteristics in the Inner Mongolia grassland of northern China. Soil Tillage Res. 150, 1–9. https://doi.org/10.1016/j.still.2014.12.019

Jarvis, N.J., Jansson, P. -E, Dik, P.E., Messing, I., 1991. Modelling water and solute transport in macroporous soil. I. Model description and sensitivity analysis. Eur. J. Soil Sci. 42, 59–70. https://doi.org/10.1111/j.1365-2389.1991.tb00091.x

Jarvis, N.J., 2007. A review of non-equilibrium water flow and solute transport in soil macropores: principles, controlling factors and consequences for water quality. Eur. J. Soil Sci. 58, 523-546. https://doi.org/10.1111/j.1365-2389.2007.00915.x

Katuwal, S., Norgaard, T., Moldrup, P., Lamandé, M., Wildenschild, D., de Jonge, L.W., 2015. Linking air and water transport in intact soils to macropore characteristics inferred from X-ray computed tomography. Geoderma 237–238, 9–20. https://doi.org/10.1016/j.geoderma.2014.08.006

Lamba, J., Way, T.R., Srivastava, P., Sen, S., Wood, C.W., Yoo, K.H., 2012. Surface transport of nutrients from surface-broadcast and subsurface-banded broiler litter. Trans. ASABE 55, 979–985. http://dx.doi.org/10.13031/2013.41530.

Luo, L., Lin, H., Halleck, P., 2008. Quantifying Soil Structure and Preferential Flow in Intact Soil Using X-ray Computed Tomography. Soil Sci. Soc. Am. J. 72, 1058–1069. https://doi.org/10.2136/sssaj2007.0179

Luo, L., Lin, H., Li, S., 2010. Quantification of 3-D soil macropore networks in different soil types and land uses using computed tomography. J. Hydrol. 393, 53–64. https://doi.org/10.1016/j.jhydrol.2010.03.031

Matthews, G.P., Laudone, G.M., Gregory, A.S., Bird, N.R.A., De, A.G., Whalley, W.R., 2010. Measurement and simulation of the effect of compaction on the pore structure and saturated hydraulic conductivity of grassland and arable soil. Water Resour. Res. 46, 1–13. https://doi.org/10.1029/2009WR007720

McGrath, G.S., Hinz, C., Sivapalan, M., Dressel, J., Pütz, T., Vereecken, H., 2010. Identifying a rainfall event threshold triggering herbicide leaching by preferential flow. Water Resour. Res. 46, 1–12. https://doi.org/10.1029/2008WR007506

Mohanty, B.P., Horton, R., Ankeny, M.D., 1996. Infiltration and macroporosity under a row crop agricultural field in a glacial till soil. Soil Sci. 161, 205–213. https://doi.org/10.1097/00010694-199604000-00001

Mooney, S.J., Morris, C., 2008. A morphological approach to understanding preferential flow using image analysis with dye tracers and X-ray Computed Tomography. Catena 73, 204–211. https://doi.org/10.1016/j.catena.2007.09.003

Müller, K., Katuwal, S., Young, I., McLeod, M., Moldrup, P., de Jonge, L.W., Clothier, B., 2018. Characterising and linking X-ray CT derived macroporosity parameters to infiltration in soils with contrasting structures. Geoderma 313, 82–91. https://doi.org/10.1016/j.geoderma.2017.10.020

Munkholm, L.J., Heck, R.J., Deen, B., 2012. Soil pore characteristics assessed from X-ray micro-CT derived images and correlations to soil friability. Geoderma 181–182, 22–29. https://doi.org/10.1016/j.geoderma.2012.02.024

Oztas, T., Koc, A., Comakli, B., 2003. Changes in vegetation and soil properties along a slope on overgrazed and eroded rangelands. J. Arid Environ. 55, 93–100. https://doi.org/10.1016/S0140-1963(02)00267-7

Perret, J., Prasher, S.O., Kanlzas, A., Langford, C., 1998. Characterization of macropore morphology in a sandy loam soil using x-ray computer assisted tomography and geostatistical analysis. Can. Water Resour. J. 23, 143–165. https://doi.org/10.4296/cwrj2302143

Phansalkar, N., More, S., Sabale, A., Joshi, M., 2011. Adaptive Local Thresholding for Detection of nuclei in diversity stained cytology images. Int. Conf. Commun. Signal Process. 218–220. https://doi.org/10.1109/ICCSP.2011.5739305

Prior, S.A., Runion, G.B., Torbert, H.A., Erbach, D.C., 2004. A hydraulic coring system for soil–root studies. Agron. J. 96:1202–1205. https://doi.org/10.2134/agronj2004.1202

Rab, M.A., Haling, R.E., Aarons, S.R., Hannah, M., Young, I.M., Gibson, D., 2014. Evaluation of X-ray computed tomography for quantifying macroporosity of loamy pasture soils. Geoderma 213, 460–470. https://doi.org/10.1016/j.geoderma.2013.08.037

Rezaei, S.A., Gilkes, R.J., 2005. The effects of landscape attributes and plant community on soil physical properties in rangelands. Geoderma 125, 145–154. https://doi.org/10.1016/j.geoderma.2004.07.011

Rueden, C.T., Schindelin, J., Hiner, M.C., DeZonia, B.E., Walter, A.E., Arena, E.T., Eliceiri, K.W., 2017. ImageJ2: ImageJ for the next generation of scientific image data. BMC Bioinformatics 18, 1–26. https://doi.org/10.1186/s12859-017-1934-z

Sen, S., Srivastava, P., Yoo, K.H., Dane, J.H., Shaw, J.N., Kang M.S., 2010. Runoff generation mechanisms in pastures of the Sand Mountain region of Alabama-a field investigation. Hydrol. Process. 14, 369-385. https://doi.org/10.1002/hyp.7502

Sen, S., Srivastava, P., Dane, J.H., Yoo, K.H., Shaw, J.N., 2010. Spatial-temporal variability and hydrologic connectivity of runoff generation areas in a North Alabama pasture-implications for phosphorus transport. Hydrol. Process. 24, 342–356. https://doi.org/10.1002/hyp.7502

Shaffer, K.A., Fritton, D.D., Baker, D.E., 1979. Drainage Water Sampling in a Wet, Dual-Pore Soil System. J. Environ. Qual. 8, 241–246. https://doi.org/10.2134/jeq1979.00472425000800020022x

Singh, P., Kanwar, R.S., Thompson, M.L., 1991. Macropore Characterization for Two Tillage Systems Using Resin-Impregnation Technique. Soil Sci. Soc. Am. J. 55, 1674–1679. https://doi.org/10.2136/sssaj1991.03615995005500060029x

Singleton, P.L., Boyes, M., Addison, B., 2000. Effect of treading by dairy cattle on topsoil physical conditions for six contrasting soil types in Waikato and Northland, New Zealand, with implications for monitoring. New Zeal. J. Agric. Res. 43, 559–567. https://doi.org/10.1080/00288233.2000.9513453

Soil Survey Staff, Natural Resources Conservation Service, United States Department of Agriculture. Web Soil Survey. Available online at the following link: http://websoilsurvey.sc.egov.usda.gov/. Accessed 20 November 2020.

Udawatta, R.P., Anderson, S.H., Gantzer, C.J., Garrett, H.E., 2008. Influence of Prairie Restoration on CT-Measured Soil Pore Characteristics. J. Environ. Qual. 37, 219–228. https://doi.org/10.2134/jeq2007.0227

Wahl, N.A., Bens, O., Buczko, U., Hangen, E., Hüttl, R.F., 2004. Effects of conventional and conservation tillage on soil hydraulic properties of a silty-loamy soil. Phys. Chem. Earth 29, 821–829. https://doi.org/10.1016/j.pce.2004.05.009

Wang, X.S., Jiang, X.W., Wan, L., Ge, S., Li, H., 2011. A new analytical solution of topography-driven flow in a drainage basin with depth-dependent anisotropy of permeability. Water Resour. Res. 47, 1–5. https://doi.org/10.1029/2011WR010507

Warner, G.S., Nieber, J.L., Moore, I.D., Geise, R.A., 1989. Characterizing Macropores in Soil by Computed Tomography. Soil Sci. Soc. Am. J. 53, 653–660. https://doi.org/10.2136/sssaj1989.03615995005300030001x

Warren, S.D., Nevill, M.B., Blackburn, W.H., Garza, N.E., 1986. Soil Response to Trampling Under Intensive Rotation Grazing. Soil Sci. Soc. Am. J. 50, 1336–1341. https://doi.org/10.2136/sssaj1986.03615995005000050050x

Watson, K.W., Luxmoore, R.J., 1986. Estimating Macroporosity in a Forest Watershed by use of a Tension Infiltrometer. Soil Sci. Soc. Am. J. 50, 578–582. https://doi.org/10.2136/sssaj1986.03615995005000030007x

Wilson, G.V., Jardine, P.M., Luxmoore, R.J., Jones, J.R., 1990. Hydrology of a Forested Hillslope during Storm Events. Geoderma 46, 119–138. https://doi.org/10.1016/0016-7061(90)90011-W

Zhang, X., Zhu, J., Wendroth, O., Matocha, C., Edwards, D., 2019. Effect of Macroporosity on Pedotransfer Function Estimates at the Field Scale. Vadose Zo. J. 18, 1–15. https://doi.org/10.2136/vzj2018.08.0151

Zhang, Y., Zhang, X., Zhang, Z., Niu, J., Zhang, M., 2017. Water flow and preferential flow: A State-of-the-Art throughout the literature. Hydrol. Earth Syst. Sci. Discuss. 1–68. https://doi.org/10.5194/hess-2017-210

Zong-Chao Li, Hu, X., Li, X.Y., Huang, Y.M., Wu, X.C., Wang, P., Liu, L.Y., 2019. Quantification of Soil Macropores at Different Slope Positions under Alpine Meadow Using Computed Tomography in the Qinghai Lake Watershed, NE Qinghai–Tibet. Eurasian Soil Sci. 52, 1391–1401. https://doi.org/10.1134/S1064229319110152

ASABE Author Information

We now use a double-blind peer review process.

Author information goes into this file, not into the manuscript file.

In ScholarOne Manuscripts, upload this file as "Other file for editors, not for reviewers."

See the ASABE website for more information for authors.

For questions 1 and 2 below, see an example in this PDF.

1. List authors, as they will appear in the article under the title. Example:

Suman Budhathoki, Jasmeet Lamba, Puneet Srivastava, Kritika Malhotra, Thomas Way, Sheela Katuwal

2. Write a paragraph with authors' names, professional titles, affiliations, affiliation addresses, email, and phone number of corresponding author. Example:

The authors are **Suman Budhathoki,** Graduate Student, **Jasmeet Lamba**, Assistant Professor, and **Kritika Malhotra**, Graduate Student, Biosystems Engineering Department, Auburn University, Auburn, Alabama, USA; **Puneet Srivastava**, Professor, College of Agriculture and Natural Resources, University of Maryland, College Park, Maryland, USA; **Thomas Way**, Agricultural Engineer, USDA-ARS National Soil Dynamics Lab Auburn, Alabama, USA; **Sheela Katuwal**, Postdoctoral Fellow, Department of Poultry Science, University of Arkansas, Fayetteville, Arkansas, USA. **Corresponding author:** Suman Budhathoki, 36830; 3345910159; email: szb0153@auburn.edu.

3. If your funding is from any of these U.S. government agencies, please complete the row.

Funder	ASABE use only	Grant or award number(s)	Is the start date after 1 January 2016? yes/no/don't know
USDA	10.13039/100000199	Award# 2018-67019-27806	Yes
NSF	10.13039/100000001		
USGS	10.13039/100000203		
USDOE	10.13039/100000015		

4. Complete a table below for each author, in the same order as the authors in question 1 above, so that their names are correctly indexed online. If there are more than six authors, copy and paste the two tables for each author. Do not change Word styles from, e.g., "Author" to "Normal" or "Affiliation" to "Normal."